Hot-melt extrudability of amorphous solid dispersions of flubendazole-copovidone: An exploratory study of the effect of drug loading and the balance of adjuvants on extrudability and dissolution

João M. C. de Assis[a], Eduardo J. Barbosa[a], Vinícius D.N. Bezzon[b], Felipe R. Lourenço[a], Flavio M.S. Carvalho[c], J.R. Matos[d]*, Nadia Araci Bou-Chacra[a], Chris J. Benmore[e], Stephen R. Byrn[f], Fanny N. Costa[g], Gabriel L. B. de Araujo[a]*

[a] Department of Pharmacy, School of Pharmaceutical Sciences, University of São Paulo (USP), São Paulo, 05508-000, SP, Brazil

[b] Center for Natural Sciences and Humanities (CCNH), Federal University of ABC (UFABC), Santo André, 09210580, SP, Brazil

[c] Geosciences Institute, Department of Mineralogy and Geotectonics, University of São Paulo (USP), São Paulo, 05508-08, SP, Brazil

[d] Department of Fundamental Chemistry, Institute of Chemistry, University of São Paulo (USP), São Paulo, 05508-000, SP, Brazil

[e] X-ray Science Division, Advanced Photon Source, Argonne National Laboratory, Illinois, 60439, United States

[f] Department of Industrial and Physical Pharmacy, Purdue University, West Lafayette, Indiana, 47906, United States

[g] Diamond Light Source, Harwell Science and Innovation Campus, Didcot, Oxfordshire, OX110DE – United Kingdon

*corresponding authors: gabriel.araujo@usp.br, jdrmatos@iq.usp.br

Abstract

The anthelmintic FDA-approved flubendazole has shown potential to be repositioned to treat cancer and dry macular degeneration, but its poor water solubility limits its use. Amorphous solid dispersions may overcome this challenge, but the balance of excipients may impact the preparation method and drug release. The purpose of this study was to evaluate the influence of adjuvants and drug loading on the development of a flubendazole-copovidone amorphous solid dispersion by hot-melt extrusion. Drug, copovidone and adjuvants (magnesium stearate and hydroxypropyl cellulose) mixtures were statistically designed, and the process performed in a twin-screw extruder. The study showed that flubendazole and copovidone mixtures were highly extrudable, except when drug loading was high (>40%). The study also showed that magnesium stearate had a positive impact on the extrusion, being more effective than hydroxypropyl cellulose. The extruded materials were evaluated by modulated differential scanning calorimetry and X-ray powder diffraction, showing positive results related to amorphization and physical stability. Pair distribution fuction analysis indicated the presence of drug-rich domains with medium-range order structure and no evidence of polymer-drug interaction. All extrudates showed faster

dissolution (HCl, pH 1.2) when compared with pure flubendazole and both adjuvants had a notable influence on the dissolution rate. In conclusion, hot-melt extrusion may be a viable option to obtain stable flubendazole:copovidone amorphous dispersions.

Keywords: flubendazole, copovidone, hydroxypropyl cellulose, magnesium stearate, hot-melt extrusion, amorphous solid dispersion, dissolution.

Abbreviations: ASD, amorphous solid dispersion; FBZ, flubendazole; HME, hot-melt extrusion; HPC, hydroxypropyl cellulose; mDSC, modulated differential scanning calorimetry; Mg St, magnesium stearate; PDF, pair distribution function; SME, specific mechanical energy; XRPD, X-ray powder diffraction.

1. Introduction

Amorphous solid dispersions (ASDs) have become a popular and efficient approach in pharmaceutical development to enhance the oral bioavailability of poorly water-soluble compounds. The amorphous drug does not have a high level of structural organization, yielding to high free energy and, consequently, increasing its solubility in the gastrointestinal medium. Therefore, the drug can reach significant levels of water solubility, allowing oral absorption (Zografi and Newman, 2016; Danda et al., 2019). ASD can improve drug bioavailability when the supersaturated state is reached and kept for enough time for the drug to be absorbed (Wilson et al., 2018).

Hot-melt extrusion (HME) is among the most efficient methods to prepare ASD (Lima et al., 2020). In this method, a carrier (usually a thermoplastic polymer) is mixed with the drug and heated at the appropriate temperature, based on the melt or glass transition temperature of the carrier selected. This process results in a solid dispersion in which the active compound is dissolved or dispersed into the polymer matrix (Tran et al., 2021). The HME process is continuous, economical, requires few steps for execution, and avoids using organic solvents and long drying periods, as required by other methods such as spray-drying (SD) (Maniruzzaman and Nokhodchi, 2017). Successfully developed products for oral administration are currently in the market, such as Kaletra® (lopinavir/ritonavir), Venclexta® (venetoclax), and Onmel® (itraconazole) (Simões et al., 2019; Solanki et al., 2019).

Considering the process, HME equipment is composed of a feeder and barrel, which contains the well-designed screws for the transporting, mixing, and meshing of the melted material. A vacuum pump can be coupled to the barrel for gases removal. In HME process, the polymer is heated until it gets to an appropriate melt viscosity, allowing drug-polymer-adjuvants to be mixed, dissolved, and extrused (Butredddy et al., 2021). The equipment is divided into zones that can be set up using different temperatures, which can be regulated for each specific formulation. At the end of the process, a die is connected to the equipment, which defines the shape of the material obtained. Parameters usually monitored include feed rate, heating zones temperature, melt pressure, extrusion torque, and screw configuration and speed (Patil et al., 2016; Tambe et al., 2021).

The working process temperature in the areas where the screws are configured with mixer elements is preferable above the melting point of the drug (T_{melt}) (Lakshman et al., 2008), and required to be 15-60 °C above the polymer glass transition temperature (T_g) (Crowley et al., 2007). This is recommended for softening the system, which improves the flow and mixing, resulting in lower torque during extrusion and better processability and dispersion at molecular level, which is essential for the enhacement of dissolution (Lakshman et al., 2008; Tambe et al., 2021). However, despite the great potential of HME process to overcome solubility problems, many drugs with high T_{melt} (above 200 °C) are challenging to extrudate (Lu et al., 2018; Huang et al., 2019), because such high temperature processing can cause drug and carriers degradation (LaFountaine et al., 2016; Haser et al., 2017; Fan et al., 2019; Huang et al., 2019).

Liu et al. (2010) highlights that, when working with high T_{melt} drug, the use of strategies for improving dispersive and distributive mixing can accelerate the amorphization process and allow to work at processing temperatures lower than the drug´s melting point (Liu et al., 2010). Ball milling (Fan et al., 2019), eutectic formation (Zhou, H. et al., 2021), supercritical carbon dioxide (Sauceau et al., 2011), pre-amorphous formation through solvent evaporation (Lakshman et al., 2008), and cocrystalization (Liu et al., 2012) are examples of sophisticated strategies that can be combined with HME to decrease extrusion processing temperatures of high T_{melt} drugs through melting point depression or suppression. More common and easily scalable approaches are the use of drug-miscible carriers and adjuvants such as plasticizers and polymer combinations to enhance processability at lower temperatures (Desai et al., 2018; Solanki et al., 2019; Zhao et al., 2019). This choice must also meet performance attributes such as dissolution, stability, and acceptable drug load to reduced dosage form size (Dedroog et al., 2019). Consequently, new systems and adjuvants are being investigated through binary and ternary mixtures to achieve better HME formulations. Maniruzzaman et al. (2012), reported the high manufacturability at low temperatures of solid lipids in extrusion processes for drug formulations (Maniruzzaman et al., 2012). Desai et al. (2018) reported the improvements in physical and mechanical properties for HME process due to the plasticizer effect of the solid lubricants polyethylene glycol 8000, stearic acid, and glyceryl behenate in indomethacin-Eudragit® E PO mixtures. The cellulose derivative hydroxypropyl cellulose (HPC), even not been largely used for HME processes, have been highlighted as a promising alternative for providing interesting properties for processability, stability and dissolution (Paradkar et al., 2009; Sarode et al., 2014; Luebbert et al., 2021). However, given the known properties of solid lipids and HPC in traditional processes of tablet development, there are concerns about the correct balance between concentration levels in formulation, dissolution, and its consequences for extrudability. Hence, it is critical to assess adjuvant and polymer characteristics in HME formulations, besides the drug:polymer miscibility and their influence on processability and dissolution.

Herein, HPC and the most popular lipid lubrificant magnesium stearate are investigated in hotmelt copovidone-based amorphous solid dispersions of flubendazole. Copovidone is a highly extrusable water-soluble thermoplastic copolymer manufactured by the polymerization of 6 parts of the hydrophilic group N-vinylpyrrolidone and 4 parts of the lipophilic monomer vinyl acetate. This amphiphilic characteristic makes copovidone a suitable polymer to be used in hot melt extrusion process as a solubilizer of poorly soluble drugs (Kolter, 2013). Flubendazole (FBZ) is a well-established anthelminthic drug that has been considered for repurposing in cancer treatment (Hou et al., 2015; Li et al., 2019; Florio et al., 2021; X. Zhou et al., 2021), besides for age-related dry macular degeneration, an irreversible cause of blindness (Zhang et al., 2021). However, reformulation is needed because FBZ is class II rated according to the Biopharmaceutics Classification System (BCS), presenting an extremely limited oral absorption due to its poor water solubility (Ceballos et al., 2012). Further, FBZ has also low solubility in the most common organic solvents; consequently, the obtention of ASD by evaporation techniques is very challenging, which makes HME such an interesting option. Unfortunately, hot melt extrusion has not been attempted due to its high T_{melt} (~238°C) (Vialpando et al., 2016). Therefore, in this study, the extrusion and dissolution properties of HME flubendazole-copovidone amorphous systems are presented, as well as the impact of potential adjuvants through the design of factorial mixtures.

2. Materials and methods

2.1. Material

FBZ was aquired from the Changzou Yabang-QH Pharmachem CO., LTD company (Changzou, Jiangsu, China). The polymers hydroxypropyl cellulose – HPC (Klucel™ EF) and copovidone (Plasdone™ S630) were kindly donated by Ashland Inc. (Wilmington, EUA). Magnesium stearate (Mg St) was aquired from Mallinckrodt Inc (St. Louis, United States).

2.2. Method

2.2.1. Experimental design for HME

The impact of FBZ, polymer and adjuvant concentrations were evaluated during the extrusion process. The design of factorial mixtures (extreme vertex type, with three components, without random curves or axial points) was evaluated through the software Minitab 17 (Minitab, Inc.). The levels of each component were chosen considering common levels reported in literature for similar studies (Desai et al., 2018; Hurley et al., 2019; Luebbert et al., 2021; Pereira et al., 2020), but also considering wide ranges for promoting variations in responses that could indicate new optimization zones. The experimental design considered 3 levels for each blend component. Copovidone was tested between the levels 60 (-1) and 90% (+1) in the formulation; the adjuvants Mg St and HPC between 0 (-1) and 20% (+1), and FBZ between 10 (-1) and 40% (+1). In case of the drug, the highest level was selected because is considered a high load for amorphous dispersion of FBZ (Vialpando et al., 2016). All experiments were performed independently. Table 1 describes the experimental matrix generated by the statistical software Minitab 17.

Table 1: Experimental matrix showing the concentrations (%w/w) of each compound. Extreme vertex, without randomized curves or axial points.

Test	FBZ (%)	Copovidone (%)	Adjuvant	
			Mg St (%)	HPC (%)
1[a]	10	90	-	-
2	10	70	20	-
3[a]	40	60	-	-
4	20	60	20	-
5	20	70	10	-
7	10	70	-	20
9	20	60	-	20
10	20	70	-	10

FBZ : flubendazole; Mg St: magnesium stearate; HPC: hydroxypropyl cellulose. [a]Note: For the sake of clarity test 6 and 8 are excluded from the table, since tests 1 & 6, 3 & 8 are the same vertex/composition of the mixture design.

2.2.2 Preparation of the solid dispersions by HME

The samples were previously weighed and mixed for 10 minutes in a V-blender (Lawes) at 15 rpm. FBZ extruded dispersions were obtained in a 18 mm twin-screw extruder with volumetric feeder, model ZSE-18 (Leistritz, Germany) (Fig. 1a). A large open die of 1.5 cm diameter was used on the process to reduce the risk of material blockage. As soon as the material left the equipment, a discharge conveyor was settled at 5 rpm to cool material down using compressed air and, to reduce extrudate diameter to be better milled (see Fig.3). For comparison purposes the process settings and screws configuration were kept constants for all experiments. To increase shear rate, thus improve distributive and dispersive drug mixing, the extruder screws were set at high speed (600 rpm) and configurated to have four zones containing kneading blocks, as shown in Fig. 1b; the screw feeder speed were set at 300 rpm to maintain a constant material throughput. The temperature of each heating zone was set above copovidone T_g on the mixing zones, as indicated in Fig. 1a. The extruded materials were milled with a conical mill (Quadro Comil) through 5.00 mm mesh, then through 2.00 mm mesh and finally 1.00 mm mesh, at 3000 rpm.

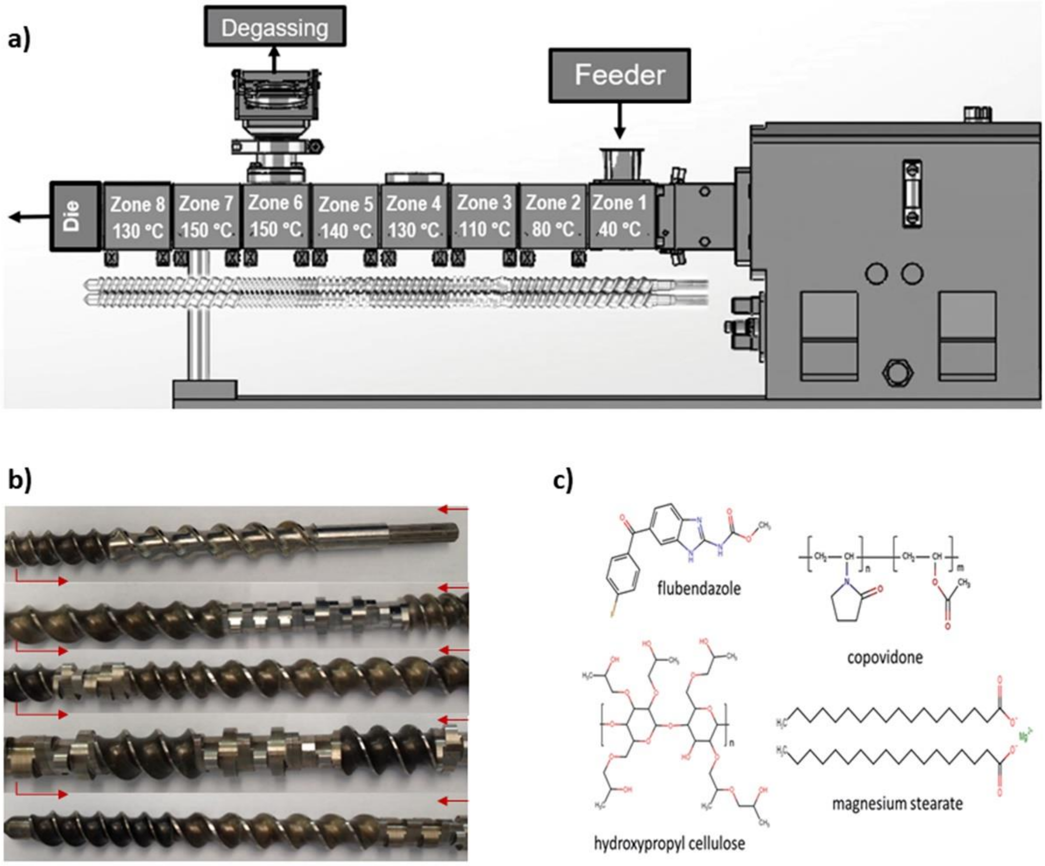

Fig. 1. Schematic of extruder Leistriz ZSE-18 (adapted with permission of Leistriz, courtesy of Charlie Martin) indicating the heating zones and their set up temperatures, co-rotating screws (source Leistritz) and extrusion flow (feeder → die) are also informed (b) screws elements used at the HME process; c) molecular structures of flubendazole, copovidone, hydroxypropyl cellulose and magnesium stearate. Structures drawn by Chemicalize (ChemAxon) (https://chemicalize.com, accessed June 2021).

2.2.3 Thermal Analysis

Differential scanning calorimetry (DSC) experiments were performed in a DSC Q2000, TA-Instruments (New Castle, DE, USA) equipment. Samples of c.a. 6 mg were scanned under dynamical nitrogen atmosphere of 50 $mL.min^{-1}$, in an aluminum pan partially closed. The glass transition temperatures were determined at heating rate of 10 $^{o}C.min^{-1}$, temperature modulation amplitude of ± 1.5 ºC; period of 40 s and temperature range between 25 and 300 ºC. For individual components and binary physical mixtures, the samples were scanned at same conditions without modulation. The equipment was previously calibrated with metallic Indium standard.

2.2.4 X-ray powder diffraction

X-ray powder diffraction (XRPD) analysis were performed for qualitative study of crystalline and amorphous phases of the extruded materials and isolated compounds. A diffractometer (Bruker) model D8 Focus, with CuK$\alpha_{1|2}$ (λ=1.5406 Å, 1.5444 Å) radiation was used. Data collection were performed in the range from 5 to 40° (2θ), with a step of 0.07° (2 θ) and 5 s/step in reflection mode.

2.2.5 Dissolution tests

The extruded samples and pure FBZ were manually encapsulated into a size 00 (Capsugel) incolor gelatine capsule, with 100 mg of drug content. Dissolution was performed using a Distek dissolution system model 2100 (Distek, NJ, USA) integrated with an Agilent 8453 in line UV/Vis (Agilent, USA), using USP apparatus I. FBZ has higher solubility at pH 1.2, because of its weakly basic nature (pKa FBZH+=3.32)(de Araujo et al., 2018); consequently, acidic medium was selected to favor dissolution. Dissolution medium was 900 mL of HCl (pH 1.2) at 37 °C ± 1 °C, set for 100 rpm rotation speed. FBZ was quantified by UV (λ = 250 nm) at time points of 5, 10, 15, 30, 45, 60, 75, 90, 105 and 120 minutes. An FBZ stock solution in formic acid (1.00 mg.mL^{-1}) was prepared and diluted with HCl to achieve linearity in the range 0.03 – 0.13 mg.mL^{-1}.

2.2.6 Pair distribution function (PDF) analysis

High-energy synchrotron X-ray powder diffraction experiments were performed at beamline 6-ID-D at the Advanced Photon Source, Argonne National Laboratory (USA), with incident energy of 100.315 keV (wavelength of 0.12360 Å). The 2D data obtained were integrated into a 1D dataset using routines within the DAWN software (Filik et al., 2017). The structure function was extracted using the PDFgetX2 software (Qiu et al., 2004 ; Juhás et al., 2013), considering a Q-range from 0.4 to 17.5 Å^{-1} for the S(Q) to perform the Fourier transform.

3. Results and discussions

3.1 Preparation of the solid dispersions by HME

HME output process parameters are summarized in Table 2 and the contour graphs of Fig. 2 show the melt pressure (a and b) and torque (c and d) for each extruded material. As the drug concentration increased in the mixture the extrusion process became more difficult, indicated by the intense rise of torque and the specific mechanical energy (SME). This was caused because the copovidone capacity to solubilize FBZ was exceeded. Consequently, the presence of undissolved solids increases the viscosity of the mixture, impairing the extrusion process. Liu et al. (2013) reported that proper solubilization of the drug in the polymer is highly dependable on the good miscibility and low viscosity of the mixture. They were able to load up to 30% of carbamazepine by combining polymers to improve processability (Liu et al., 2013). In our case, the extrusion of the high drug load test 3 (40% FBZ) reached 100% torque and exceeded the maximal pressure tolerated by the equipment (>2,000 psi), resulting in obstruction of the melted material at the exit of the extruder. A test 3 sample (40:60 FBZ:copovidone) recovered from the obstructed equipment is shown in Fig. 3. The opacity of this sample indicated that FBZ was undissolved, i.e., the drug remained in a crystalline state, which was confirmed by XRPD analysis (not shown).

Table 2: HME output process parameters for the tested formulations.

Test	Torque (%)	Residence time (s)	Melt pressure (psi)	Feeding rate for 300 rpm (kg.h^{-1})	SME** (kWh.kg^{-1})
1	48	53	186	1.14	1.9196
2	17	63	212	0.78	0.9936
3	>100	not evaluated	>2000 psi*	not evaluated	not evaluated
4	20	75	200	0.60	1.5197
5	24	47	189	0.96	1.1398
7	57	52	191	0.74	3.5117
9	66	58	186	0.61	4.9327
10	65	55	174	0.83	3.5703

* When the pressure meter (located at the end of the equipment) reaches pressure level equal to or above 2000 psi, it causes the extruder to emit an alert signal. Then, the process is interrupted until the pressure is decreased at lower levels. Same happens when torque reaches 100%. ** SME: Specific mechanical energy.

The contour graphs (Fig. 2) were plotted to better visualize the impact of each compound concentration in the extrusion process. The increase of the drug concentration and the reduction of copovidone negatively interfere with FBZ extrusion process. However, combinations with Mg St (2, 4 and 5) significantly improved processability, being more effective than HPC rich formulations (7, 9 and 10), which presented the highest specific energy and torque values (Table 2). The difference between Mg St and HPC may be related to the structural difference between the adjuvants (Fig. 1b): while Mg St has a lipophilic characteristic, HPC does not have the lubricant effect as strong as Mg St, despite its hydrophilic structure suitable for drug:polymer interactions in ASD. Besides the well described lubricant effect of Mg St in HME (Pereira et al., 2020), the efficiency is also related to the solubilization and miscibility of FBZ in the melted Mg St. This was confirmed by complementary DSC analysis of a FBZ:Mg St binary physical mixture (1:1 ratio), in which it was possible to observe the Mg St melting at 108 °C (T_{onset}) and the subsequent absence of FBZ melting peak at 246 °C (Supplementary Material, Fig.S1A). Regarding to

FBZ:HPC binary mixture (1:1 ratio), the FBZ melting peak was maintained, indicating no detectable interaction between both (Supplementary Material, Fig.S1B). Despite Klucel™ EF is widely used in HME due to its lower viscosity and lower processing temperature (Jani and Patel, 2015), which improves processability, this was not effective in the case of FBZ. Repka et al. (2000) also reported issues during processing of HME films due to the excessive stress caused by HPC in the formulation (Repka and McGinity, 2000).

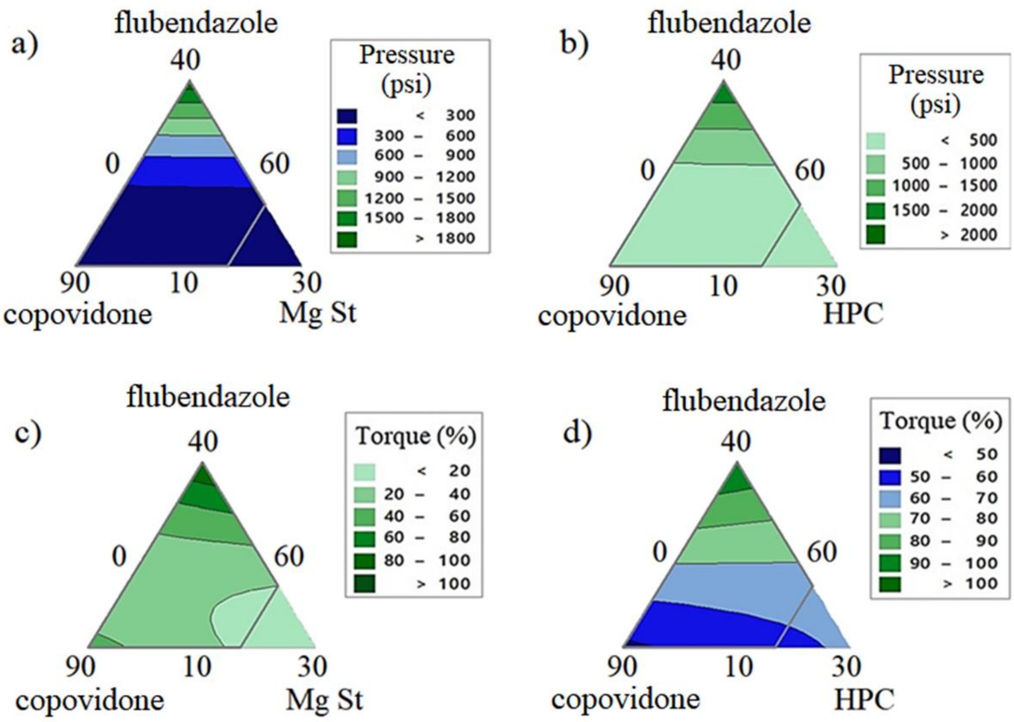

Fig. 2. Contour graph of melt pressure (a and b) and torque (c and d) for the mixtures FBZ:copovidone:adjuvant. Maximum pressure and torque of 2000 psi and 100%, respectively, were used as criteria. Values in the countor graphics represent the proportion (%, w/w) in the formulation. Mg St: magnesium stearate; HPC: hydroxypropyl cellulose.

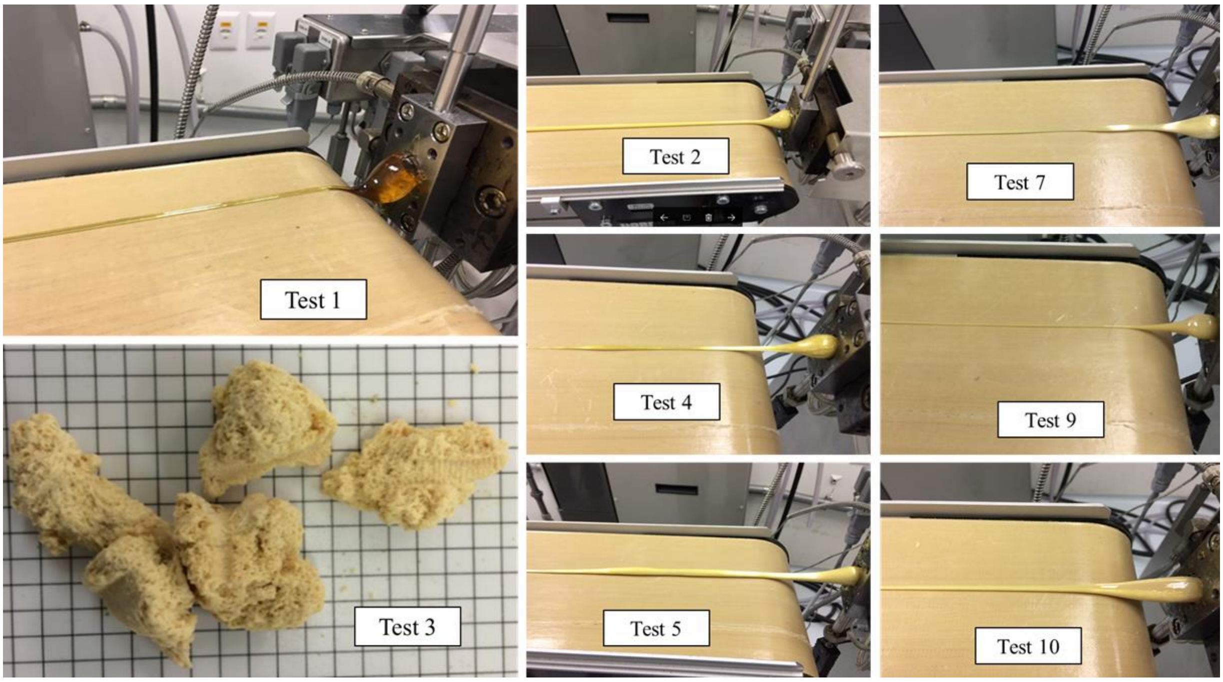

Fig. 3. HME samples obtained from the equipment: 1: 10:90 flubendazole:copovidone mixture; 2, 4 and 5: samples with magnesium stearate; 7, 9 and 10: samples with hydroxypropyl cellulose. Test 3 sample (40:60 flubendazole:copovidone) obtained from obstructured equipment. Its opacity indicates that the drug was undissolved, which was confirmed by XRPD analysis (data not shown).

3.3 Thermal analysis

Fig. 4 shows DSC curves of the extruded materials (tests 1, 4 and 9) and the isolated components. FBZ melts at 246 °C and Mg St at 122 °C. The copovidone already in the amorphous state does not present any endothermic event related to fusion. In this case, only an event attributed to T_g can be observed. For all the extruded materials, the peak of FBZ fusion was absent indicating a disarranged of the crystalline packing and, in such a way, the molecules of this drug came out randomly dispersed, that is the condition of amorphous systems. The success of amorphization is related to the interaction between the active pharmaceutical ingredient (API) and carriers (polymers and adjuvants). The intermolecular interactions between functional groups of the carrier and the drug, as dipole-dipole interactions, Van der Waals and hydrogen bonds, have a central role to keep the active substance into an amorphous state. Such interactions increase the miscibility of the drug with the polymeric matrix and maintain the stability of the drug into an amorphous state or molecularly dispersed. (Kaushal et al., 2004; Qian et al., 2010). The other thermal event observed in Test 1 sample was the T_g of amorphous FBZ, remaining at the average value of 160°C, as indicated in Fig. 4D. For the other tests, this event could not be detected by the analysis parameters selected. The presence of two T_g's demonstrate that the system formed by copovidone and amorphous FBZ have two distinct phases. This is an indication of amorphous phase separation and despite of fact that the sample is amorphous by conventional X-ray Powder Diffraction Amorphous (see section 3.4), the system is heterogeneous and may contain the presence of drug-rich domains in which recrystallization may start (Lin and Huang, 2010). Thus, further investigation with PDF analysis was performed and it is discussed below (see section 3.6).

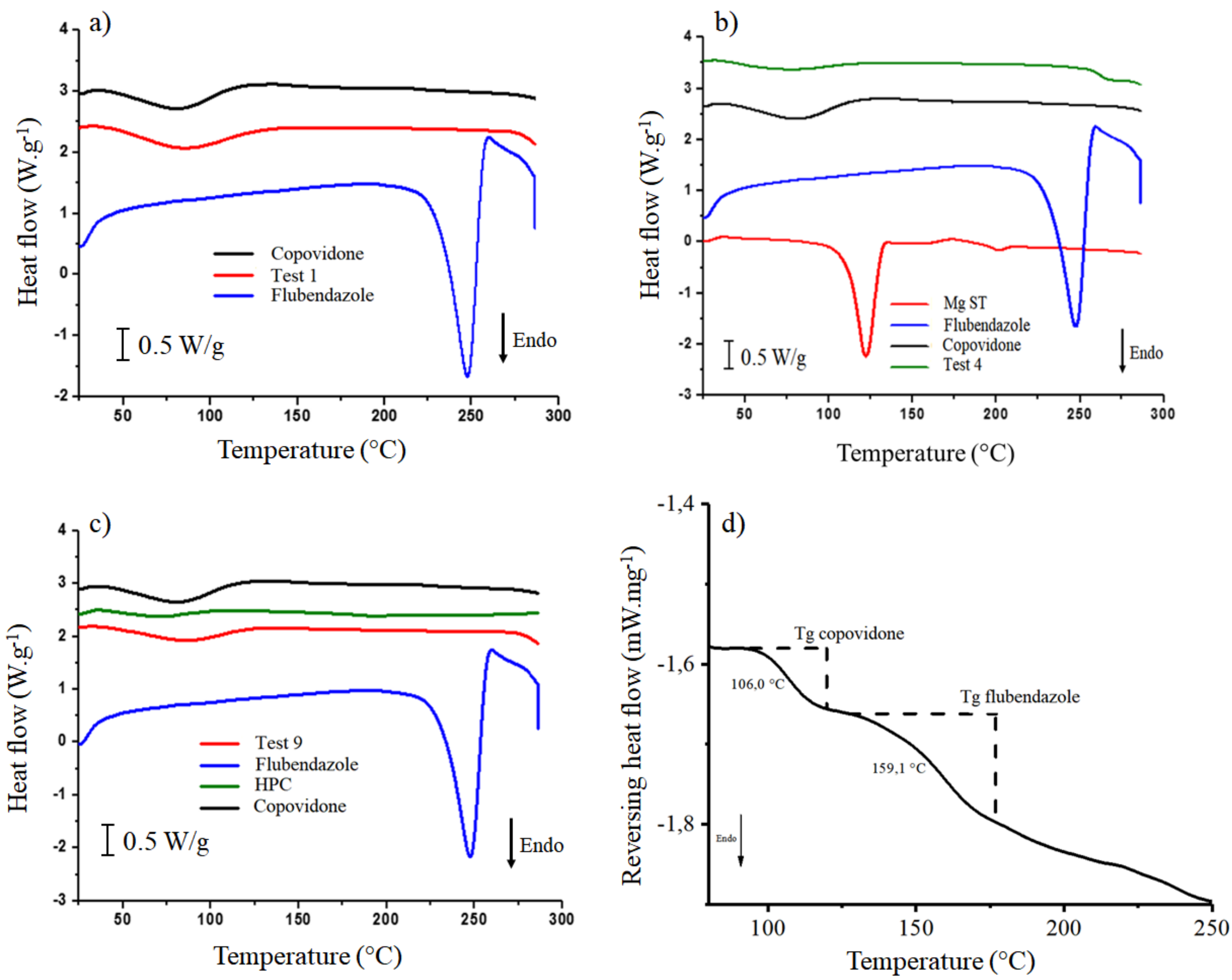

Fig. 4. DSC curve for tests 1, 4, 9, and the isolated components flubendazole, Mg St and HPC (a, b, c); d) mDSC curve (reversing heat flow signal) for test 1, emphasizing the event of vitreous transition of copovidone (106 °C) and flubendazole (159 °C). All the curves obtained through dynamical atmosphere of N_2 (50 mL.min^{-1}) and heating rate of 10 °C.min^{-1}.

3.4 X-ray powder diffraction data

The samples were analyzed by X-ray powder diffractometry to confirm the amorphous nature of the FBZ amorphous solid dispersion. The diffractograms of the initial extruded materials and isolated components of the formulations are indicated in Fig. 5a. FBZ crystalline structure presents Bragg peaks around 6° and 17° (2θ). A similar result has been reported (Vigh et al., 2017), which indicates the initial crystalline state of pure FBZ. Mg St in its turn presents typical peaks around 5° and 9° (2θ), besides a large peak around 21° (2θ). This pattern may be assigned to the anhydrate phase, but the two peaks around 21° (2θ) may indicate a hydrate phase (Bracconi et al., 2003). Thus, it is possible that the Mg St used could contain a small fraction of magnesium stearate hydrate phase. Since Mg St melts at the same temperature range expected for the water loss, consequently, the water loss event is not clearly observed in the DSC. The detection of the presence of hydrate by thermal analysis may be better visualized by using thermogravimetry in complementary investigations.These results confirm the hypothesis that the crystalline materials were amorphous after HME, since any peak of the FBZ or Mg St crystalline compounds is observed. The extruded materials were also evaluated after 12 months at room temperature and no recrystallization was observed (Fig. 5b) by the conventional XRPD analysis..

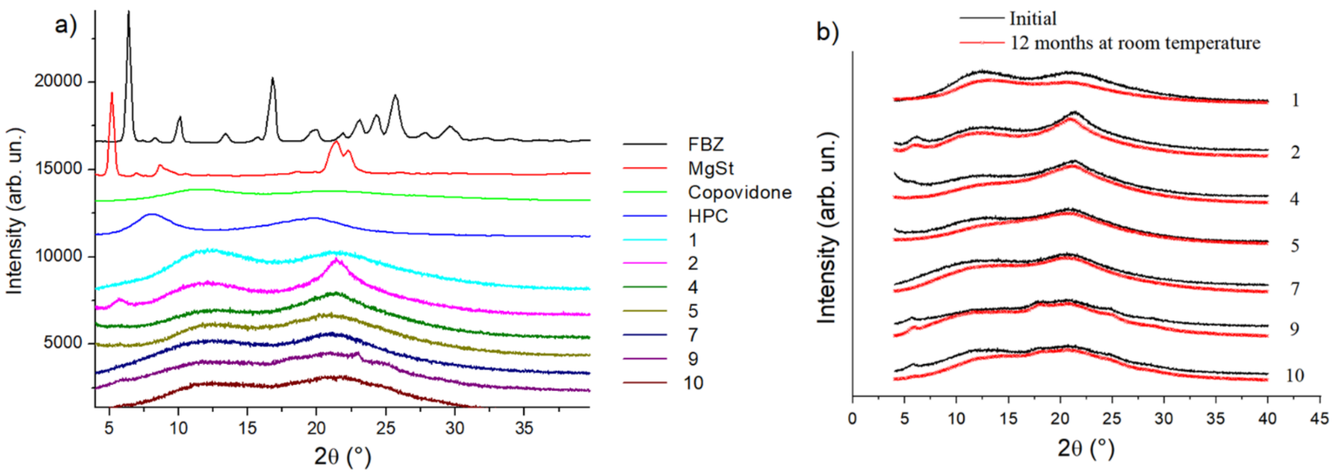

Fig. 5. Diffractograms of the extruded materials. a) initial. b) after 12 months of stability study at room temperature. 1: 10:90 flubendazole:copovidone mixture; 2, 4 and 5: samples with magnesium stearate; 7, 9 and 10: samples with hydroxypropyl cellulose.

3.5 Dissolution tests

Dissolution profiles of extruded materials *versus* pure FBZ are showed in Fig. 6 (a), where 100% is the complete dissolution of a 100 mg dose of the API. The time for capsule disintegration varied, leading to a high relative standard deviation (RSD) at the initial points of the experiment. Tests 2, 4, 5, 9, 10 and pure FBZ presented residual material at the last time of collection, which also contributed for a higher deviation. FBZ release (%) and RSD results are presented in supplementary material.

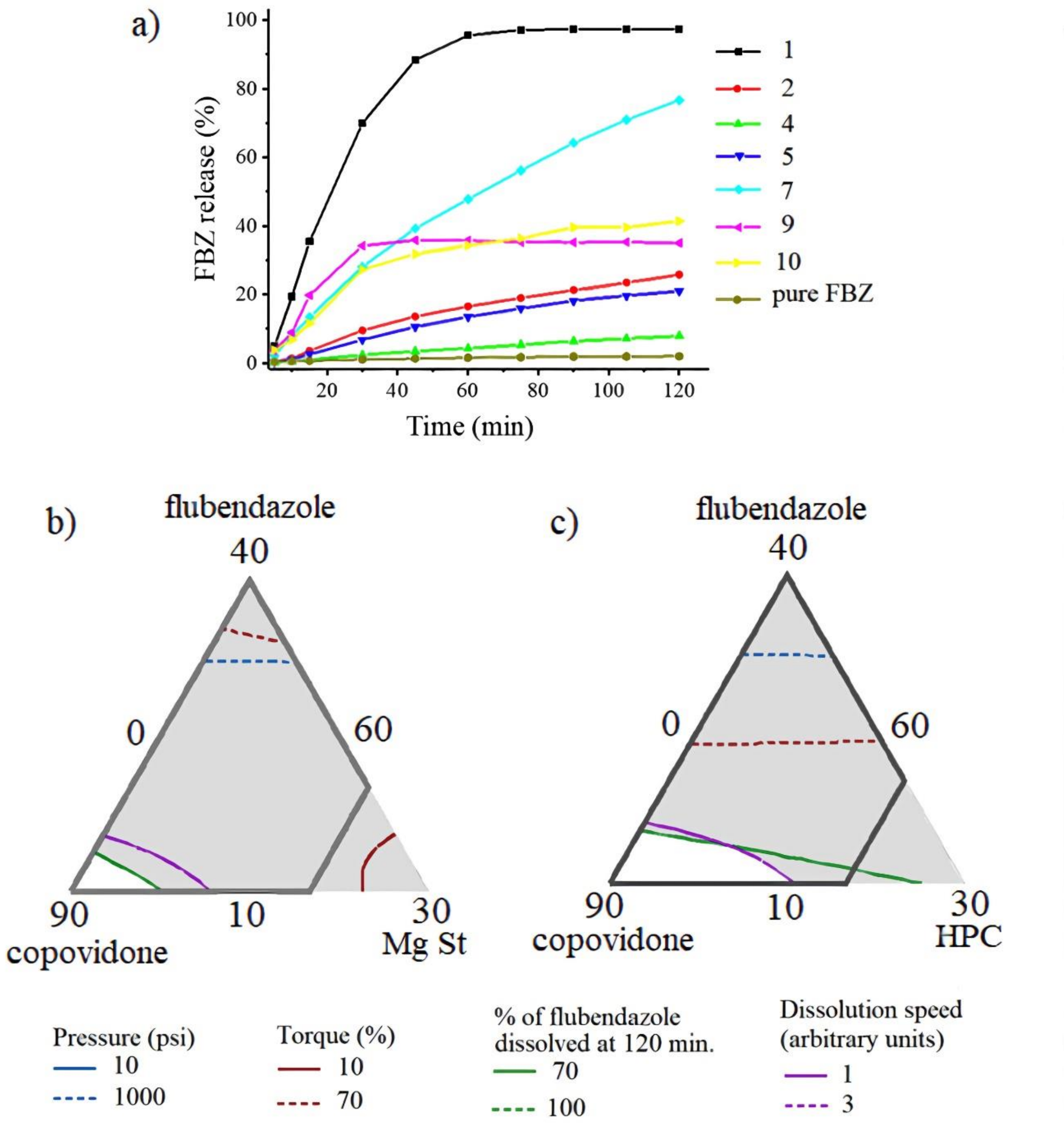

Fig. 6. a) Dissolution profiles of extruded materials versus pure FBZ, realized through HCl pH 1.2, at 37 °C (± 1°C), apparatus I (100 rpm), collecting times 5, 10, 15, 30, 45, 60, 75, 90, 105 and 120 minutes. 1: 10:90 flubendazole:copovidone mixture; 2, 4 and 5: samples with magnesium stearate; 7, 9 and 10: samples with hydroxypropyl cellulose. b) and c) Contour graph of melt pressure, torque, dissolution and dissolution speed for the FBZ:copovidone mixtures with Mg St (b) and HPC (c). Values in the countor graphics represent the proportion (%, w/w) in the formulation. Satisfactory values for the responses: pressure between 10 and 1000 (psi), torque between 10 and 70 (%), dissolution at 120 min between 70 and 100%, and dissolution speed between 1 and 3 (arbitrary units). The white region is where these conditions are met.

We noticed a faster and significant increase of FBZ ASD dissolution compared with the pure crystalline drug, regardless of the formulation. As soon as copovidone is increased and the adjuvant reduced, FBZ release increases. Furthermore, rising drug load had a negative effect on FBZ dissolution. Among the extruded materials, test 1 (10:90 FBZ:copovidone) showed the best FBZ release per unit time. However, this formulation did not provide the best processability for HME (Table 2). Besides, in part, the project was aimed at optimizing drug loading, but HME of test 3 (40:60 FBZ:copovidone) failed due to its high melt viscosity, which leads to equipment obstruction. Hence, reducing drug load could allow FBZ:copovidone ASD extrusion and provide the best release results with no need of adjuvant. Nevertheless, we evaluated the addition of Mg St or HPC and the balance of FBZ:copovidone HME process and dissolution performance. For this purpose, FBZ HME contour graphs (Fig 6b and c), were considered satisfactory values for the responses: melted material pressure between 10 and 1000 (psi), torque between 10 and 70 (%), drug dissolution between 70% and 100% at 120 min., and dissolution speed between 1 and 3 (arbitrary units).

According to the results, the impact of Mg St on the dissolution profile was greater than HPC due to its high hydrophobicity, which hinders the penetration of the dissolution media through the granules of the extruded material. This phenomenon might be attributed to the formation of a hydrophobic film around the particles and reduced wettability (Wang et al., 2010; Zarmpi et al., 2020). In fact, formulations with Mg St (2, 4 and 5) provided the best processability for HME (Table 2), but release results were only better than pure FBZ. Since we used Mg St concentrations of 20, 20 and 10% (tests 2, 4 and 5, respectively), the proportion of this lubricant should be lowered to maintain the improved processability, compared with test 1 (10:90 FBZ:copovidone). Therefore, test 5 (20:70:10 FBZ:copovidone:Mg St) has twice the FBZ drug load compared with test 1, and provided the best processability and release results when using Mg St. We hypothesize that in futher opmization experiments reducing lubricant to a concentration as small as possible could maintain the improved processability, while dissolution would be as good as test 1. However, the contour graph in Fig. 6b shows that the ideal conditions to achieve at least 70% of dissolution at 120 min. are in the white region. It means that copovidone proportion would have to be close to 90%, and FBZ and Mg St as small as possible, which approximates the condition of the test 1. Therefore, increasing FBZ has a negative impact on dissolution, whereas Mg St improves processability but compromises drug release.

Sarode et al. 2014 reported that the use of HPC in ASD preparations produced by hot melt mixing can enhance dissolution properties of felodipine (Sarode et al., 2014). In our case for HPC, formulation 7 (10:70:20 FBZ:copovidone:HPC) provided the release result after 2h that most closely achieved that obtained with test 1, despite slower release rate and incomplete dissolution (< 80%). The contour graph in Fig. 6c shows that the ideal conditions to achieve at least 70% FBZ release are similar to those when using Mg St, except that it is possible to use higher proportions of HPC compared to Mg St. HPC is widely used as carrier for HME due to its suitable properties such as relatively high T_g (which can inhibit recrystallization during storage) and melting viscosity (suitable for processing) (Luebbert et al., 2021; Sarode et al., 2014). However, the addition of this polymer did not improve processability (Table 2) nor significantly enhanced dissolution to justify its use. Therefore, the results herein obtained did not indicate the need of the adjuvants for FBZ ASD HME.

3.6 Pair distribution function analysis

It is known that due to Scherrer broadening, the conventional XRPD analysis is not able to identify nanocrystalline domains that may trigger crystallization (Billinge, 2019). Another point to be considered is the low crystalline quantity that can be identified considering the limit of resolution of the equipment set up using to perform the measurements. In our case, conventional XRPD analysis for test 1 did not indicate any crystalline/nanocrystalline domains, i.e., by this analysis test 1 sample was X-ray amorphous. However, thermal analysis indicated the presence of amorphous phase separation, i.e. the presence of two T_g's demonstrate that the system formed by copovidone and amorphous FBZ have two distinct phases (Lin and Huang, 2010). Thus, Pair Distribution Function analysis was used to investigate the local structure of the dispersion and confirm the presence of locally well-ordered drug-rich domains, being crystalline and/or nanocrystalline ones.

Figure 7a shows the structure factor S(Q) for pure copovidone and test 1 samples. Copovidone S(Q) does not have any crystalline Bragg peaks, indicating the amorphous structure for the sample. However, test 1 S(Q) has subtle peaks mainly before 4 $Å^{-1}$, which can be related to crystalline domains in the system. Notably, these crystalline domains could not be observed in the conventional X-ray diffraction pattern, demonstrating the high sensibility to small crystalline contributions that high-resolution X-ray diffraction presents. Also, domains smaller than 30 nm are not detected by DSC (Newman et al., 2008). In figure 7b are presented the PDF pattern for the test 1 sample (black), scaled Copovidone PDF pattern at 90%(blue), scaled crystalline FBZ PDF pattern at 10% (green) and the result composition (red) between the pure compounds (Copovidone and FBZ) scaled at the proportion that is expect for the test 1 sample (10:90 FBZ:Copovidone). The PDF pattern based on the proportion of the compounds (red line) agrees with that one for the pure test 1 pattern indicating that small poorly formed crystals (of a few nm in size) appear to be trapped in the polymer at 10% concentration.

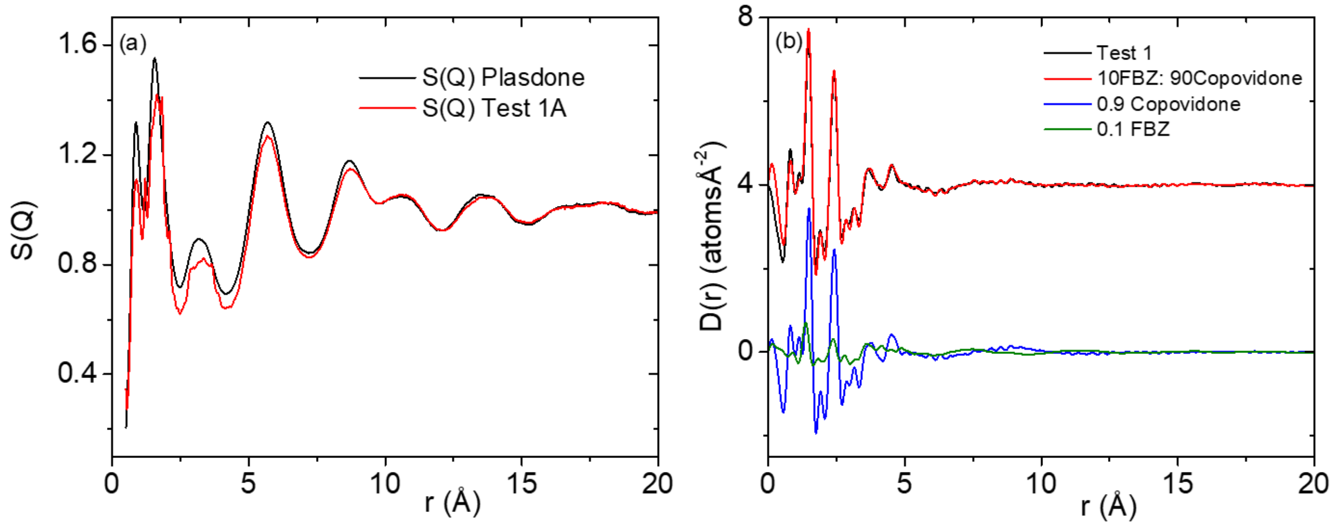

Fig. 7: (a) Structure function S(Q) obtained for pure copovidone and test 1; (b) PDF function for the test 1 (10:90 flubendazole:copovidone), pure flubendazole (crystalline) scaled at 10%, pure copovidone scaled at 90% and the composition between scaled copovidone and flubendazole patterns.

Possible interaction between drug and matrix was also evaluated by the PDF method and the result are presented in Figure 8. In this analysis, the intermediate range order of the test 1 sample minus the polymer matches the intermolecular packing of FBZ (red line), which indicates there does not seem to be any evidence of a significant polymer-drug interaction. Therefore, the results presented in this section, along with stability results show that there are no crystalline peaks in the test 1 sample after 12 months, which suggests that the matrix preserved the small formed crystals/nanocrystals, which stay trapped in the system avoiding in its turn complete drug recrystallization.

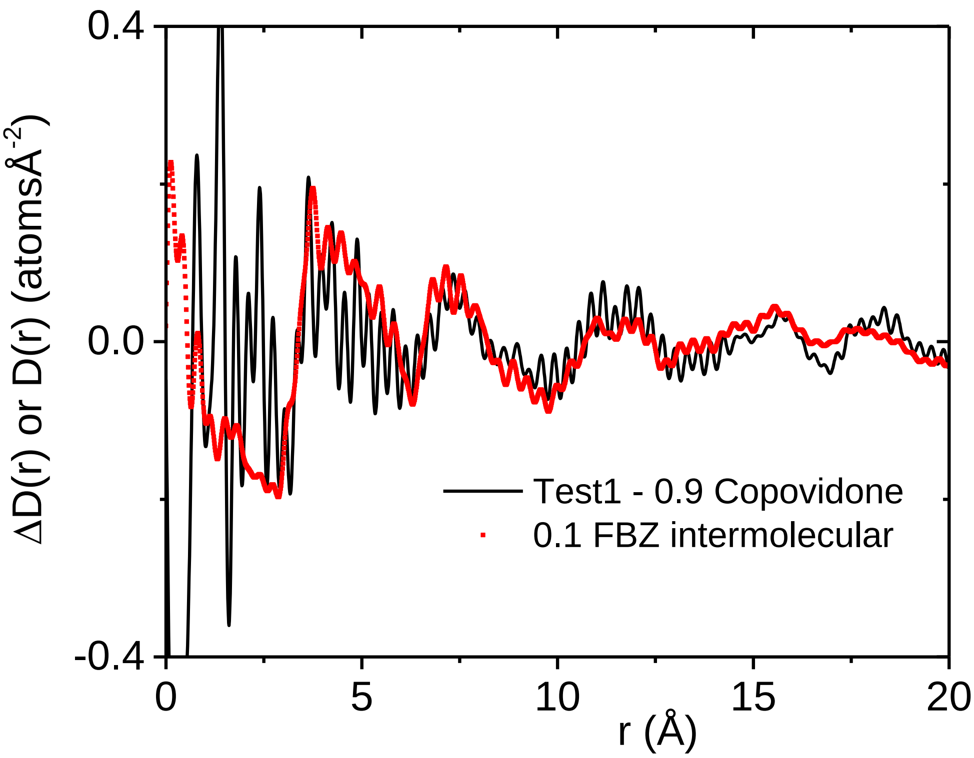

Fig. 8: Subtraction polymer correlations from the test 1 sample correlations result in the intermediate range order that matches intermolecular packing of flubendazole.

4. Conclusion

In this study we investigated the influence of flubendazole and copovidone concentrations as well as the impact of potential adjuvants MgSt and HPC on the processability and dissolution of HME ASD formulations. Flubendazole and copovidone had a strong influence on the success of the extrusions. Based on the dissolution endpoint of 70% drug dissolved, the study showed the best concentration range of each material. Countour diagrams were used to show the ranges of melt pressure and torque that led to the optimum dissolution rate. MgSt can improve processability, being more effective than HPC rich formulations, however, its use compromises dissolution. On the other hand, HPC can increase release at certain level; however, adjuvant free formulation had the best FBZ release. DSC and X-ray analysis of the extruded material indicated the absence of crystallinity for all produced and viable extruded material, but the presence of drug-rich domains (phase separation) was indicated by glass transition determination and PDF analysis. The compositions remained stable for 12 months at room temperature. This study showed that hot melt extrusion of flubendazole-copovidone compositions can be optimized to give products with acceptable dissolution.

5. Acknowledgments

The authors thank the financial support of São Paulo Research Foundation (FAPESP) grants #2018/11990-5 and 2019/04998-2. This study was financed in part by the Coordenação de Aperfeiçoamento de Pessoal de Nível Superior - Brasil (CAPES) - Finance Code 001. Ashland Inc. (Wilmington, USA) is acknowledged for the donation of raw materials and for supporting with the use of hot-melt extrusion facilities. The authors also thank the Advanced Photon Source Synchrotron for the measurement using this facility. The Advanced Photon Source is operated for the U.S. Department of Energy (DOE) Office of Science by Argonne National Laboratory and supported by the U.S. DOE under Contract No. DE-AC02-06CH11357.

References

Bezzon, V.D.N., Ferreira, F.F., Smith, P., Benmore, C.J., Byrn, S.R., de Araujo, G.L.B., 2021. Amorphous dispersions of flubendazole in hydroxypropyl methylcellulose: Formulation stability assisted by pair distribution function analysis. International Journal of Pharmaceutics, v.600, 120500. https://doi.org/10.1016/j.ijpharm.2021.120500

Billinge, S.J., 2019. The rise of the X-ray atomic pair distribution function method: a series of fortunate events. Philosophical Transactions of the Royal Society A 377, 20180413. https://doi.org/10.1098/rsta.2018.0413

Bracconi, P., Andrès, C., Ndiaye, A., 2003. Structural properties of magnesium stearate pseudopolymorphs: effect of temperature. International Journal of Pharmaceutics, v.262, 109-124. https://doi.org/10.1016/S0378-5173(03)00339-9

Butreddy, A., Bandari, S., Repka, M.A., 2021. Quality-by-design in hot melt extrusion based amorphous solid dispersions : An industrial perspective on product development. European Journal of Pharmaceutical Sciences, v.158, 105655. https://doi.org/10.1016/j.ejps.2020.105655

Ceballos, L., Moreno, L., Torrado, J.J., Lanusse, C., Alvarez, L., 2012. Exploring flubendazole formulations for use in sheep. Pharmacokinetic evaluation of a cyclodextrin-based solution. BMC veterinary research, v.8, 71. https://doi.org/10.1186/1746-6148-8-71

Craig, D.Q., 2002. The mechanisms of drug release from solid dispersions in water-soluble polymers. International Journal of Pharmaceutics, v.231, 131–144.

https://doi.org/10.1016/S0378-5173(01)00891-2

Crowley, M.M., Zhang, F., Repka, M.A., Thumma, S., Upadhye, S.B., Kumar Battu, S., McGinity, J.W., Martin, C., 2007. Pharmaceutical applications of hot-melt extrusion: part I. Drug development and industrial pharmacy 33, 909–926. https://doi.org/10.1080/03639040701498759

Danda, L.J.A., Batista, L.M., Melo, V.C.S., Sobrinho, J.L.S., Soares, M.F. de L.R., 2019. Combining amorphous solid dispersions for improved kinetic solubility of posaconazole simultaneously released from soluble PVP/VA64 and an insoluble ammonio methacrylate copolymer. European Journal of Pharmaceutical Sciences, v.133, 79–85. https://doi.org/10.1016/j.ejps.2019.03.012

de Araujo, G.L., Benmore, C.J., Byrn, S.R., 2017. Local structure of ion pair interaction in lapatinib amorphous dispersions characterized by synchrotron x-ray diffraction and pair distribution function analysis. Scientific Reports 7. https://doi.org/10.1038/srep46367

Dedroog, S., Huygens, C, Mooter, G.V., 2019. Chemically identical but physically different: A comparison of spray drying, hot melt extrusion and cryo-milling for the formulation of high drug loaded amorphous solid dispersions of naproxen. European Journal of Pharmaceutics and Biopharmaceutics, v.135, 1-12. https://doi.org/10.1016/j.ejpb.2018.12.002

Desai, D., Sandhu, H., Shah, N., Malick, W., Zia, H., Phuapradit, W., Vaka, S.R.K., 2018. Selection of Solid-State Plasticizers as Processing Aids for Hot-Melt Extrusion. Journal of Pharmaceutical Sciences, v.107, 372-379. https://doi.org/10.1016/j.xphs.2017.09.004

Entrocasso, C., Alvarez, L., Manazza, J., Lifschitz, A., Borda, B., Virkel, G., Mottier, L., Lanusse, C., 2008. Clinical efficacy assessment of the albendazole–ivermectin combination in lambs parasitized with resistant nematodes. Veterinary Parasitology, v.155, 249–256. https://doi.org/10.1016/j.vetpar.2008.04.015

Fan, W., Zhu, W., Zhang, X., Xu, Y., Di, L., 2019. Application of the combination of ball-milling and hot-melt extrusion in the development of an amorphous solid dispersion of a poorly water-soluble drug with high melting point. RSC advances 9, 22263–22273. https://doi.org/10.1039/C9RA00810A

Filik, J., Ashton, A.W., Chang, P.C.Y., Chater, P.A., Day, S.J., Drakopoulos, M., Gerring, M.W., Hart, M.L., Magdysyuk, O.V., Michalik, S., Smith, A., Tang, C.C., Terrill, N.J., Wharmby, M.T., Wilhelm, H., 2017. Processing two-dimensional X-ray diffraction and small-angle scattering data in DAWN 2. Journal of Applied Crystallography, v.50, 959 —966. https://doi.org/10.1107/S1600576717004708

Florio, R., Carradori, S., Veschi, S., Brocco, D., De Genni, T., Cirilli, R., Casulli, A., Cama, A., De Lellis, L., 2021. Screening of Benzimidazole-Based Anthelmintics and Their Enantiomers as Repurposed Drug Candidates in Cancer Therapy. Pharmaceuticals, v.14, 372. https://doi.org/10.3390/ph14040372

Haser, A., Huang, S., Listro, T., White, D., Zhang, F., 2017. An approach for chemical stability during melt extrusion of a drug substance with a high melting point. International journal of pharmaceutics 524, 55–64. https://doi.org.10.1016/j.ijpharm.2017.03.070

Hou, Z.-J., Luo, X., Zhang, W., Peng, F., Cui, B., Wu, S.-J., Zheng, F.-M., Xu, J., Xu, L.-Z., Long, Z.-J., 2015. Flubendazole, FDA-approved anthelmintic, targets breast cancer stem-like cells. Oncotarget, v.6, 6326. https://doi.org/10.18632/oncotarget.3436

Huang, D., Xie, Z., Rao, Q., Liamas, E., Pan, P., Guan, S., Zhang, Z.J., Lu, M., Li, Q., 2019. Hot melt extrusion of heat-sensitive and high melting point drug: Inhibit the recrystallization of the prepared amorphous drug during extrusion to improve the bioavailability. International Journal of Pharmaceutics, v.565, 316-324. https://doi.org/10.1016/j.ijpharm.2019.04.064

Hurley, D., Carter, D., Ng, L.Y.F., Davis, M., Walker, G.M., Lyons, J.G., Higginbotham, C.L., 2019. An investigation of the inter-molecular interaction, solid-state properties and dissolution properties of mixed copovidone hot-melt extruded solid dispersions. Journal of Drug Delivery Science and Technology 53, 101132. https://doi.org/10.1016/j.jddst.2019.101132

Jani, R., Patel, D., 2015. Hot melt extrusion: An industrially feasible approach for casting orodispersible film. Asian Journal of Pharmaceutical Sciences, v.10, 292–305. https://doi.org/10.1016/j.ajps.2015.03.002

Juhás, P., Davis, T., Farrow, C.L., Billinge, S.J.L., 2013. PDFgetX3 : a rapid and highly automatable program for processing powder diffraction data into total scattering pair distribution functions. Journal of Applied Crystallography, v.46, 560–566. https://doi.org/10.1107/S0021889813005190

Kaushal, A.M., Gupta, P., Bansal, A.K., 2004. Amorphous drug delivery systems: molecular aspects, design, and performance. Critical Reviews™ in Therapeutic Drug Carrier Systems, v.21, 133-193. https://doi.org/10.1615/critrevtherdrugcarriersyst.v21.i3.10

Kolter, K., 2013. Properties and applications of polyvinyllactam polymers, in: Melt Extrusion. Springer, pp. 83–105.

LaFountaine, J.S., McGinity, J.W., Williams, R.O., 2016. Challenges and strategies in thermal processing of amorphous solid dispersions : a review. AAPS PharmSciTech 17, 43–55.

https://doi.org/10.1208/s12249-015-0393-y

Lakshman, J.P., Cao, Y., Kowalski, J., Serajuddin, A.T., 2008. Application of melt extrusion in the development of a physically and chemically stable high-energy amorphous solid dispersion of a poorly water-soluble drug. Molecular pharmaceutics 5, 994–1002. https://doi.org/10.1021/mp8001073

Leuner, C., Dressman, J., 2000. Improving drug solubility for oral delivery using solid dispersions. European journal of Pharmaceutics and Biopharmaceutics, v.50, 47–60. https://doi.org/10.1016/S0939-6411(00)00076-X

Li, Y., Acharya, G., Elahy, M., Xin, H., Khachigian, L.M., 2019. The anthelmintic flubendazole blocks human melanoma growth and metastasis and suppresses programmed cell death protein-1 and myeloidderived suppressor cell accumulation. Cancer Letters, v.459, 268-276. https://doi.org/10.1016/j.canlet.2019.05.026

Lima, A.L., Pinho, L.A., Chaker, J.A., Sa-Barreto, L.L., Marreto, R.N., Gratieri, T., Gelfuso, G.M., Cunha-Filho, M., 2020. Hot-Melt Extrusion as an Advantageous Technology to Obtain Effervescent Drug Products. Pharmaceutics, v.12, 779. https://doi.org/10.3390/pharmaceutics12080779

Lin, D., Huang, Y., 2010. A thermal analysis method to predict the complete phase diagram of drug–polymer solid dispersions. International journal of pharmaceutics 399, 109–115. https://doi.org/10.1016/j.ijpharm.2010.08.013

Liu, H., Wang, P., Zhang, X., Shen, F., Gogos, C.G., 2010. Effects of extrusion process parameters on the dissolution behavior of indomethacin in Eudragit® E PO solid dispersions. International journal of pharmaceutics 383, 161–169. https://doi.org/10.1016/j.ijpharm.2009.09.003

Liu, J., Cao, F., Zhang, C., Ping, Q., 2013. Use of polymer combinations in the preparation of solid dispersions of a thermally unstable drug by hot-melt extrusion. Acta Pharmaceutica Sinica B, v.3, 263–272. https://doi.org/10.1016/j.apsb.2013.06.007

Liu, X., Lu, M., Guo, Z., Huang, L., Feng, X., Wu, C., 2012. Improving the chemical stability of amorphous solid dispersion with cocrystal technique by hot melt extrusion. Pharmaceutical research 29, 806–817. https://doi.org/10.1007/s11095-011-0605-4

Lu, J., Obara, S., Ioannidis, N., Suwardie, J., Gogos, C., Kikuchi, S., 2018. Understanding the Processing Window of Hypromellose Acetate Succinate for Hot-Melt Extrusion, Part I: Polymer Characterization and Hot-Melt Extrusion. Advances in Polymer Technology, v.37, 21652. https://doi.org/10.1002/adv.21652

Luebbert, C., Stoyanov, E., Sadowski, G., 2021. Phase behavior of ASDs based on hydroxypropyl cellulose. International journal of pharmaceutics: X 3, 100070. https://doi.org/10.1016/j.ijpx.2020.100070

Maniruzzaman, M., Boateng, J.S., Snowden, M.J., Douroumis, D., 2012. A review of hot-melt extrusion: process technology to pharmaceutical products. International Scholarly Research Notices 2012. https://doi.org/10.5402/2012/436763

Maniruzzaman, M., Nokhodchi, A., 2017. Continuous manufacturing via hot-melt extrusion and scale up: regulatory matters. Drug Discovery Today, v.22, 340-351. https://doi.org/10.1016/j.drudis.2016.11.007

Newman, A., Engers, D., Bates, S., Ivanisevic, I., Kelly, R.C., Zografi, G., 2008. Characterization of amorphous API: polymer mixtures using X-ray powder diffraction. Journal of pharmaceutical sciences 97, 4840–4856. https://doi.org/10.1002/jps.21352

Paradkar, A., Kelly, A., Coates, P., York, P., 2009. Shear and extensional rheology of hydroxypropyl cellulose melt using capillary rheometry. Journal of pharmaceutical and biomedical analysis 49, 304–310. https://doi.org/10.1016/j.jpba.2008.11.014

Patil, H., Tiwari, R.V., Repka, M.A., 2016. Hot-Melt Extrusion : from Theory to Application in Pharmaceutical Formulation. AAPS PharmSciTech, v.17, 20-42. https://doi.org/10.1208/s12249-015-0360-7

Pereira, G.G., Figueiredo, S., Fernandes, A.I., Pinto, J.F., 2020. Polymer selection for hot-melt extrusion coupled to fused deposition modelling in pharmaceutics. Pharmaceutics, v.12, 795. https://doi.org/10.3390/pharmaceutics12090795

Qian, F., Huang, J., Hussain, M.A., 2010. Drug–polymer solubility and miscibility: stability consideration and practical challenges in amorphous solid dispersion development. Journal of pharmaceutical sciences, v. 99, 2941–2947. https://doi.org/10.1002/jps.22074

Qiu, X., Thompson, J.W., Billinge, S.J.L., 2004. PDFgetX2: a GUI-driven program to obtain the pair distribution function from X-ray powder diffraction data. Journal of Applied Crystallography, v.37, 678. https://doi.org/10.1107/S0021889804011744

Repka, M.A., McGinity, J.W., 2000. Physical–mechanical, moisture absorption and bioadhesive properties of hydroxypropyl cellulose hot-melt extruded films. Biomaterials, v.21, 1509–1517. https://doi.org/10.1016/S0142-9612(00)00046-6

Sarode, A.L., Malekar, S.A., Cote, C., Worthen, D.R., 2014. Hydroxypropyl cellulose stabilizes amorphous solid dispersions of the poorly water soluble drug felodipine. Carbohydrate Polymers, v.112, p.512-519. https://doi.org/10.1016/j.carbpol.2014.06.039

Sauceau, M., Fages, J., Common, A., Nikitine, C., Rodier, E., 2011. New challenges in polymer foaming: A review of extrusion processes assisted by supercritical carbon dioxide. Progress in Polymer Science 36, 749–766. https://doi.org/10.1016/j.progpolymsci.2010.12.004

Simões,M.F., Pinto, R.M.A., Simões, S., 2019. Hot-melt extrusion in the pharmaceutical industry: toward filing a new drug application. Drug Discovery Today, v.24, 1749-1768. https://doi.org/10.1016/j.drudis.2019.05.013

Solanki, N.G., Lam, K., Tahsin, M., Gumaste, S.G., Shah, A.V., Serajuddin, A.T., 2019. Effects of surfactants on itraconazole-HPMCAS solid dispersion prepared by hot-melt extrusion I: miscibility and drug release. Journal of pharmaceutical sciences 108, 1453–1465. https://doi.org/10.1016/j.xphs.2018.10.058

Svensson, S.O., Hanfland, M., Fitch, A.N., Hausermann, D., 1996. Two-dimensional detector software: From real detector to idealised image or two-theta scan AU - Hammersley, A. P. High Pressure Research, v.14, 235–248. https://doi.org/10.1080/08957959608201408

Tambe, S., Jain, D., Agarwal, Y., Amin, P., 2021. Hot-melt extrusion: highlighting recent advances in pharmaceutical applications. Journal of Drug Delivery Science and Technology 102452. https://doi.org/10.1016/j.jddst.2021.102452

Tian, Y., Jacobs, E., Jones, D.S., McCoy, C.P., Wu, H., Andrews, G.P., 2020. The design and development of high drug loading amorphous solid dispersion for hot-melt extrusion platform. International Journal of Pharmaceutics, v.586, 119545. https://doi.org/10.1016/j.ijpharm.2020.119545

Tran, P.H.L., Lee, B.J., Tran, T.T.D., 2021. Recent studies on the processes and formulation impacts in the development of solid dispersions by hot-melt extrusion. European Journal of Pharmaceutics and Biopharmaceutics, v.164, 13-19. https://doi.org/10.1016/j.ejpb.2021.04.009

Vialpando, M., Smulders, S., Bone, S., Jager, C., Vodak, D., Van Speybroeck, M., Verheyen, L., Backx, K., Boeykens, P., Brewster, M.E., 2016. Evaluation of three amorphous drug delivery technologies to improve the oral absorption of flubendazole. Journal of pharmaceutical sciences, v.105, 2782–2793. https://doi.org/10.1016/j.xphs.2016.03.003

Vigh, T., Démuth, B., Balogh, A., Galata, D.L., Assche, I.V., Mackie, C., Vialpando, M., Hove, B.V., Psathas, P., Borbás, E., Pataki, H., Boeykens, P., Marosi, G., Verreck, G., Nagy, Z.K., 2017. Oral bioavailability enhancement of flubendazole by developing nanofibrous solid dosage forms. Drug Development and Industrial Pharmacy, v.43, 1126-1133. https://doi.org/10.1080/03639045.2017.1298121

Wang, J., Wen, H., Desai, D., 2010. Lubrication in tablet formulations. European Journal of Pharmaceutics and Biopharmaceutics, v.75, 1-15. https://doi.org/10.1016/j.ejpb.2010.01.007

Wilson, V., Lou, X., Osterling, D.J., Stolarik, D.F., Jenkins, G., Gao, W., Zhang, G.G., Taylor, L.S., 2018. Relationship between amorphous solid dispersion in vivo absorption and in vitro dissolution: phase behavior during dissolution, speciation, and membrane mass transport. Journal of Controlled Release, v.292, 172–182. https://doi.org/10.1016/j.jconrel.2018.11.003

Zarmpi, P., Flanagan, T., Meehan, E., Mann, J., Fotaki, N., 2020. Impact of Magnesium Stearate Presence and Variability on Drug Apparent Solubility Based on Drug Physicochemical Properties. The AAPS Journal, v.22, 75. https://doi.org/10.1208/s12248-020-00449-w

Zhang, Q., Presswalla, F., Ali, R.R., Zacks, D.N., Thompson, D.A., Miller, J.M.L., 2021. Pharmacologic activation of autophagy without direct mTOR inhibition as a therapeutic strategy for treating dry macular degeneration. Aging-US, v.13, 10866-10890. https://doi.org/10.18632/aging.202974

Zhao, Yanna, Xie, X., Zhao, Yuping, Gao, Y., Cai, C., Zhang, Q., Ding, Z., Fan, Z., Zhang, H., Liu, M., 2019. Effect of plasticizers on manufacturing ritonavir/copovidone solid dispersions via hot-melt extrusion: Preformulation, physicochemical characterization, and pharmacokinetics in rats. European Journal of Pharmaceutical Sciences 127, 60–70. https://doi.org/10.1016/j.ejps.2018.10.020

Zhou, H., Wang, Y., Li, S., Lu, M., 2021. Improving chemical stability of resveratrol in hot melt extrusion based on formation of eutectic with nicotinamide. International Journal of Pharmaceutics 607, 121042. https://doi.org/10.1016/j.ijpharm.2021.121042

Zhou, X., Zou, L., Chen, W., Yang, T., Luo, J., Wu, K., Shu, F., Tan, X., Yang, Y., Cen, S., Li, C., Mao, X., 2021. Flubendazole, FDA-approved anthelmintic, elicits valid antitumor effects by targeting P53 and promoting ferroptosis in castration-resistant prostate cancer. Pharmacological Research, v.164, 105305. https://doi.org/10.1016/j.phrs.2020.105305

Zografi, G., Newman, A., 2016. Interrelationships Between Structure and the Properties of Amorphous Solids of Pharmaceutical Interest. Journal of Pharmaceutical Sciences, v.106, 5-27. https://doi.org/10.1016/j.xphs.2016.05.001